The Journal of Immunology, 2025, **00**, 1–17
https://doi.org/10.1093/jimmun/vkaf050
Research Article

Comprehensive analysis of immune checkpoint molecules profiles phenotype and function of exhausted T cells in enzootic bovine leukosis

Hayato Nakamura[1], Satoru Konnai[1,2,3,4,*], Tomohiro Okagawa[2], Naoya Maekawa[2], Wisa Tiyamanee[1], Mari Ikehata[1], Koume Matsubara[1], Kei Watari[1], Kana Kamitani[5], Maya Saito[5], Yukinari Kato[6], Yasuhiko Suzuki[2,3,7,8], Shiro Murata[1,2,4], and Kazuhiko Ohashi[1,2,4,9]

[1]Department of Disease Control, Faculty of Veterinary Medicine, Hokkaido University, Sapporo, Japan
[2]Department of Advanced Pharmaceutics, Faculty of Veterinary Medicine, Hokkaido University, Sapporo, Japan
[3]Institute for Vaccine Research and Development (HU-IVReD), Hokkaido University, Sapporo, Japan
[4]Veterinary Research Unit, International Institute for Zoonosis Control, Hokkaido University, Sapporo, Japan
[5]Hokkaido Hayakita Meat Inspection Center, Hokkaido Government, Abira, Japan
[6]Department of Antibody Drug Development, Tohoku University Graduate School of Medicine, Sendai, Japan
[7]Division of Bioresources, International Institute for Zoonosis Control, Hokkaido University, Sapporo, Japan
[8]Global Station for Zoonosis Control, Global Institution for Collaborative Research and Education (GI-CoRE), Hokkaido University, Sapporo, Japan
[9]International Affairs Office, Faculty of Veterinary Medicine, Hokkaido University, Sapporo, Japan

*Corresponding author: Department of Disease Control, Faculty of Veterinary Medicine, Hokkaido University, Sapporo, Japan. Email: konnai@vetmed.hokudai.ac.jp

Abstract

Bovine leukemia virus (BLV) causes enzootic bovine leukosis (EBL), a B-cell lymphoma in cattle. Previous studies have demonstrated that T cells of BLV-infected cattle show increased expression of immune checkpoint molecules, including programmed death-1 (PD-1), lymphocyte-activation gene-3 (LAG-3), cytotoxic T-lymphocyte-associated antigen-4 (CTLA-4), and T-cell immunoglobulin domain and mucin domain-3 (TIM-3), leading to T-cell exhaustion. However, the key immune checkpoint molecules driving T-cell exhaustion in BLV-induced tumorigenesis remained unclear. In this study, we identified the key immune checkpoint molecules by performing comprehensive flow cytometric analyses of T cells from EBL cattle, and elucidated the phenotype and function of exhausted T cells using a transcriptomic analysis by RNA sequencing and cell culture assays. The comprehensive expression analysis revealed that the proportion of $CD4^+$ and $CD8^+$ T cells co-expressing PD-1 and TIM-3 was significantly increased in the peripheral blood and tumor tissues of EBL cattle compared to healthy cattle. Transcriptomic analysis of PD-1^+TIM-3^+ T cells revealed the upregulation of genes related to terminal exhaustion and the downregulation of genes related to T-cell differentiation and response in this subset. Additionally, PD-1^+TIM-3^+ T cells exhibited higher expression of CTLA-4, LAG-3, and Eomes, and lower expression of T-bet, suggesting a terminally exhausted phenotype. Cell culture assays revealed a significant impairment in IFN-γ production in PD-1^+TIM-3^+ T cells upon stimulation, reflecting severe dysfunction. These findings indicate that PD-1^+TIM-3^+ T cells play a central role in T-cell exhaustion during BLV-induced tumorigenesis. This study provides valuable insights for future therapeutic strategies against BLV infection.

Keywords: immunodeficiency diseases, large animals, T cells, tumor immunity, viral

Introduction

Bovine leukemia virus (BLV) is a retrovirus that induces B-cell lymphoma development in cattle, which is known as enzootic bovine leukosis (EBL),[1,2] resulting in the formation of lymphomas in lymph nodes and non-lymphatic organs, as well as leukemia in most cases.[3] Although viral factors and the host immune response contribute to the progression of EBL,[4,5] the specific mechanisms for its pathogenesis remain unclear. Despite extensive studies into the pathogenesis of BLV infection, there is still no available effective vaccine or treatment, and the number of EBL cases continues to increase worldwide, including in Japan.[6] During the disease progression in BLV infection, T cells eventually lose their function, leading to the exhaustion of the T-cell response. In BLV-infected cattle, persistent lymphocytosis (PL) is represented by an increased number of B cells in the blood with reduced expression of Th1 cytokines, such as IFN-γ, compared with alymphocytotic (AL) cattle.[7,8] Immune checkpoint molecules have been linked as key contributors to T-cell exhaustion during BLV infection.[9]

Our previous studies have revealed that the expression levels of immune checkpoint molecules such as programmed death-1 (PD-1),[10,11] PD-ligand 1 (PD-L1),[12] T-cell immunoglobulin and mucin domain-3 (TIM-3),[13,14] cytotoxic T-lymphocyte-associated antigen-4 (CTLA-4),[15] and lymphocyte-activation gene-3 (LAG-3)[16,17] are elevated in BLV-infected cattle. These molecules are important regulators of immune exhaustion, participating in T-cell dysfunction, viral persistence, and disease progression in human patients and mouse models of chronic infections and cancers.[18–20] The increased expression of these immune checkpoint molecules following persistent antigenic stimulation and inflammation results in T-cell exhaustion that is characterized by a reduced Th1 response and decreased cellular proliferation.[19,20] Additionally, blocking these immune checkpoint molecules with specific antibodies could activate bovine T cells.[11,12,14,17,21,22]

Received: October 24, 2024. **Accepted:** February 26, 2025

However, clinical trials revealed that the treatment using an anti-PD-L1 or anti-PD-1 blocking antibody was insufficient to reduce the proviral load in BLV-infected cattle with high proviral load.[23,24] Therefore, it is crucial to perform a comprehensive analysis of exhausted T cells during BLV infection and develop a therapeutic strategy targeting multiple immune checkpoints to achieve more effective therapeutic outcomes and control of BLV infection.

In human patients and mouse models of cancers, T cells expressing multiple immune checkpoints often present with a terminally exhausted phenotype that manifests as diminished effector function and an inability to respond to antigenic stimulation.[25,26] These terminally exhausted T cells are differentiated from a progenitor exhausted population, which has preserved some proliferative capacity.[27,28] The transcription factors such as T-bet and Eomes play opposing roles in regulating T-cell exhaustion: T-bet enhances T-cell function and suppresses immune checkpoint expression,[29] whereas Eomes promotes immune dysfunction by upregulating immune checkpoint molecules.[30] As T cells progress from a progenitor to a terminal exhausted subset, T-bet expression decreases, while Eomes expression increases, worsening immune dysfunction.[31,32] Despite the well-established roles of immune checkpoint molecules in T-cell exhaustion in humans and mice, the detailed mechanisms of T-cell exhaustion in cattle, particularly in BLV-infected cattle, remain unknown. Previous studies in cattle have primarily focused on one or two immune checkpoint molecules and individually assessed their contribution to T-cell exhaustion.[10–17] Furthermore, a comprehensive evaluation of multiple immune checkpoint molecules in T cells from BLV-infected cattle has not been performed.

This study aimed to elucidate the profile of exhausted T cells in EBL cattle by analyzing the co-expression of multiple immune checkpoint molecules. Furthermore, the phenotype and function of exhausted T-cell subsets expanded in EBL were characterized, uncovering the distinct features of this population.

Materials and methods

Bovine blood and tumor samples

Peripheral blood from clinically healthy adult cattle (Holstein breed) was collected at the Field Science Center for the Northern Biosphere, Hokkaido University (Sapporo, Hokkaido, Japan) and dairy farms in Hokkaido, Japan. Normal lymph nodes were collected from healthy adult cattle that showed no abnormal signs, including tumor formation, during necropsy at the Hokkaido Hayakita Meat Inspection Center (Abira, Hokkaido, Japan). Peripheral blood, lymph nodes, and various solid organs from adult cattle diagnosed with lymphoma (Holstein breed, Japanese Black breed, and crossbreed) were also collected at Meat Hygiene Inspection Centers and Livestock Hygiene Service Centers in Japan. All samples were submitted for analysis within 2 d after collection. This animal experiment was approved by the Ethics Committee of the Faculty of Veterinary Medicine, Hokkaido University (approval numbers 17-0024 and 22-0038).

To separate WBCs, whole blood was lysed with ammonium-chloride-potassium lysis buffer (154 mM ammonium chloride, 12 mM potassium bicarbonate, and 0.11 mM EDTA). Lymphoma samples were minced into small pieces with scissors and fitered through a 40-μm cell strainer (BD Biosciences, Franklin Lakes, New Jersey, USA) to obtain single-cell suspensions. The cells were washed twice with PBS supplemented with 0.5 mg/mL disodium EDTA (Dojindo Molecular Technologies, Kumamoto, Japan) and analyzed.

Diagnosis of BLV infection and EBL onset

BLV infection was confirmed by the detection of BLV provirus in DNA specimens extracted from WBCs or tissue cells using quantitative real-time PCR using a LightCycler 480 System II (Roche Diagnostics, Mannheim, Germany) with a BLV detection kit (TaKaRa Bio, Kusatsu, Japan) as described previously.[33] BLV-associated lymphomas were further evaluated via histopathological examination. EBL cattle were defined as cattle manifesting lymphomas or leukemia accompanied by clonal expansion of BLV-infected cells. The clonal expansion was confirmed using the clonality analysis by RAISING as described previously.[33] Phenotyping of tumor cells in lymph nodes and non-lymphoid organs from EBL cattle was conducted following a previous protocol that was slightly modified by using Alexa Flour 647–conjugated anti-human CD79a mAb (HN57, Bio-Rad, Hercules, California, USA) and FITC-conjugated anti-human CD3 mAb (CD3-12, Bio-Rad) for intracellular staining to determine B- and T-cell populations.[34]

Analysis of immune checkpoint molecule expression by flow cytometry

The expression of PD-1, TIM-3, CTLA-4, and LAG-3 on $CD4^+$ and $CD8^+$ T cells was analyzed in WBCs and single cells from tissue specimens by flow cytometry utilizing the antibodies shown in Table S1 and Fig. S1. To prevent nonspecific binding to Fc receptors, WBCs (1×10^6) or tissue-derived single cells (5×10^6) were pretreated with PBS containing 10% inactivated goat serum (Thermo Fisher Scientific, Waltham, Massachusetts, USA) at 25 °C for 15 min. The cells were then incubated with primary mAbs against bovine PD-1, TIM-3, CTLA-4, and LAG-3 or corresponding isotype control antibodies at 25 °C for 20 min. The anti-bovine PD-1, CTLA-4, and LAG-3 mAbs used in this study were generated as previously described.[24,35,36] Anti-bovine TIM-3 mAb (1D3-A6, mouse IgG_1, Fig. S1) was biotinylated using the Zenon Biotin Mouse IgG_1 Labeling Kit (Thermo Fisher Scientific) before incubation with the cells. This antibody was newly generated in this study and validated as shown in Fig. S1 and detailed in the Supplemental Materials and Methods.[37] After washing, the cells were stained with appropriate fluorochrome-labeled secondary antibodies and streptavidin at 25 °C for 20 min. Subsequently, the cells were stained with anti-bovine CD3, CD4, and CD8 mAbs and Fixable Viability Dye eFluor 780 (Thermo Fisher Scientific) at 25 °C for 20 min. PBS containing 0.5% bovine serum albumin (Sigma-Aldrich, St. Louis, Missouri, USA), 2 mM disodium EDTA (Dojindo Molecular Technologies), and 0.1% sodium azide (Sigma-Aldrich) was used for antibody dilution and cell washing. Following the final wash, the cells were immediately analyzed using an LSRFortessa flow cytometer (BD Biosciences). Data analysis was conducted using FlowJo v10.4 software (BD Biosciences). The gating strategies for each cell population are presented in Fig. S2.

The staining of PD-1, TIM-3, CTLA-4, and LAG-3 on γδ T cells was conducted by the method described above, with a specific modification for γδTCR detection using anti-bovine TcR1-N24 (δ chain) mAb (GB21A, Washington State University

Monoclonal Antibody Center, Pullman, Washington, USA). The detailed staining panel for γδ T cells is provided in Table S1. The stained cells were immediately analyzed using the SA3800 (Sony, Tokyo, Japan), and the gating strategies are described in Fig. S8.

Phenotypic analysis of PD-1$^+$TIM-3$^+$ T cells

To evaluate exhausted T cells, surface staining was similarly conducted using the antibodies shown in Table S1. Single cells (5×10^6) from lymphomas formed in the lymph nodes of EBL cattle were pretreated with PBS containing 10% inactivated goat serum (Thermo Fisher Scientific) at 25 °C for 15 min. The cells were then incubated with primary mAbs against bovine PD-1 and TIM-3 or corresponding isotype control antibodies at 25 °C for 20 min. After washing, the cells were incubated with fluorochrome-conjugated secondary antibodies and streptavidin at 25 °C for 20 min. The cells were then stained with fluorochrome-conjugated mAbs against CD4, CD8, CD69, CD25, and CD3 and LIVE/DEAD Fixable Olive (557) Viability Kit (Thermo Fisher Scientific). For intracellular staining, the cells were fixed and permeabilized using the BD Cytofix/Perm Kit (BD Biosciences). Intracellular staining of T-bet, Eomes, and CD3 was conducted using the conjugated mAbs listed in Table S1 at 25 °C for 20 min. After staining, the cells were immediately analyzed by flow cytometry using a spectral cell analyzer SA3800 (Sony, Tokyo, Japan).

Cell sorting

PD-1$^+$TIM-3$^+$ T cells were isolated from dissociated lymph nodes of EBL cattle. To block nonspecific binding, lymph node cells (1×10^9) were pretreated with PBS containing 10% inactivated goat serum (Thermo Fisher Scientific) at 25 °C for 15 min. The cells were then incubated with anti-bovine CD3 mAb (MM1A, Washington State University Monoclonal Antibody Center) at 25 °C for 30 min and incubated with anti-mouse IgG_1 microbeads (Miltenyi Biotec, Bergisch Gladbach, Germany) and PerCp/Cy5.5-conjugated anti-mouse IgG goat antibody (BioLegend, San Diego, California, USA) at 25 °C for 30 min. CD3$^+$ T cells were then enriched using MS columns (Miltenyi Biotec). After magnetic enrichment, the cells were stained for bovine PD-1 and TIM-3 at 25 °C for 20 min and incubated with fluorochrome-conjugated primary mAbs against bovine CD4 and CD8, fluorochrome-conjugated secondary antibodies, and Fixable Viability Dye eFluor 780 (Thermo Fisher Scientific) at 25 °C for 20 min (Table S1). Matched isotype controls were used for negative control staining. The stained cells were immediately sorted into double-positive (DP; PD-1$^+$TIM-3$^+$) and non-double-positive (non-DP; PD-1$^-$TIM-3$^-$, PD-1$^+$TIM-3$^-$, or PD-1$^-$TIM-3$^+$) T cells using a FACSAria II flow cytometer (BD Biosciences). The purity of sorted DP and non-DP cells among CD4$^+$ or CD8$^+$ T cells was typically greater than 90% and at least 85%, as confirmed by postsort analysis.

RNA sequencing

Total RNA was extracted from each sorted cell fraction using Direct-zol RNA Miniprep Kit (Zymo Research, Irvine, California, USA). Non-stranded RNA sequencing (RNA-seq) libraries were prepared using SMART-Seq v4 Ultra Low Input RNA Kit (Takara Bio). Sequencing was carried out on an Illumina NovaSeq X Plus (2 × 150–bp paired-end reads) and generated 2 × 13.3 million raw paired-end reads per library. Raw data of RNA-seq were quality checked by using FastQC version 0.11.9, and trimming was conducted using fastp version 20.1. Mapping was performed with Salmon version 1.10.0 using the ARS-UCD1.3 cDNA index for cattle. Transcript quantification data were imported into R version 4.4.2 using the tximport package, and differential gene expression analysis was conducted with DESeq2. Volcano plots displayed differentially expressed genes (DEGs) between DP and non-DP cell fractions for both CD4$^+$ and CD8$^+$ T cells, with significance thresholds set at $\log_2$ (fold change) $> |1|$ and adjusted P-value < 0.05. Heat maps showed the relative expression (z-score) of the top 60 upregulated and downregulated genes in DP CD4$^+$ and CD8$^+$ T cells. Gene Set Enrichment Analysis (GSEA) of DP CD4$^+$ and CD8$^+$ T cells was conducted using KEGG pathway gene sets, comparing gene expression data from DP T cells with the combined data from other fractions. Pathways with false discovery rate (FDR) <0.25 were defined as enriched. KEGG pathway analysis was performed to illustrate functional enrichment of genes increased or decreased in DP CD4$^+$ and CD8$^+$ T cells, using a significance threshold of adjusted P-value <0.05.

Cell culture

Isolated T-cell fractions were suspended in RPMI 1640 medium (Sigma-Aldrich) supplemented with 10% heat-inactivated FBS (Thermo Fisher Scientific), 200 IU/mL of penicillin (Thermo Fisher Scientific), 200 μg/mL of streptomycin (Thermo Fisher Scientific), and 2 mM L-glutamine (Thermo Fisher Scientific). The cells were then cultured in triplicate at 37 °C in 5% CO_2 either with 1 μg/mL anti-bovine CD3 mAb (MM1A, Washington State University Monoclonal Antibody Center) and 1 μg/mL anti-bovine CD28 mAb (CC220, Bio-Rad) for 72 h, or with 20 ng/μL phorbol 12-myristate 13-acetate (PMA; FUJIFILM Wako Pure Chemical, Osaka, Japan) and 1 μg/mL ionomycin (Sigma-Aldrich) for 18 h. After incubation, IFN-γ concentrations in culture supernatants were evaluated in duplicate using the bovine IFN-γ ELISA Development Kit (Mabtech, Nacka Strand, Sweden). Absorbance was measured at 450 nm using a microplate reader MTP-900 (Corona Electric, Tokyo, Japan).

Statistics

Statistical analysis was conducted using R version 4.3.1. The Mann–Whitney U test was used to compare the expression levels of immune checkpoint molecules in the peripheral blood between EBL and healthy cattle. The Steel-Dwass test was applied for multiple-group comparisons of the expression levels of immune checkpoint molecules in the lymph nodes and non-lymphoid organs. The Wilcoxon signed-rank test was used to analyze the exhausted T-cell phenotypes and IFN-γ production from CD3/CD28-stimulated T cells. A paired t test (one-tailed) was conducted to evaluate the statistical significance of IFN-γ production from PMA/ionomycin-stimulated T cells, which were cultured in triplicate. Spearman rank correlation was used for the correlation analysis. P-values of less than 0.05 were considered significant.

Data availability

The RNA-seq data are available from the DDBJ Sequence Read Archive under the accession number PRJDB20193. All datasets used and analyzed in this study are available from the corresponding author upon reasonable request.

Results

Expression profile of immune checkpoint molecules is altered in the peripheral blood of EBL cattle

We developed a multicolor staining panel for flow cytometry to detect PD-1, TIM-3, CTLA-4, and LAG-3 on $CD4^+$ and $CD8^+$ T cells in order to comprehensively assess the expression of immune checkpoint molecules on T cells from EBL cattle (Fig. S2). Flow cytometry analysis revealed distinct changes in the expression profiles of immune checkpoint molecules on the peripheral blood T cells between healthy and EBL cattle (Fig. 1A–D). To visualize the expression landscape of immune checkpoint molecules in healthy and EBL cattle, T cells were divided into 5 groups based on the number of positive immune checkpoint molecules in each cell: negative, single-, double-, triple-, and quadruple-positive (Fig. 1A). In EBL cattle, the population of $CD4^+$ and $CD8^+$ T cells expressing 2, 3, or 4 immune checkpoint molecules were more frequent than that in healthy cattle, whereas the single-positive population was smaller (Fig. 1A). Among the single-positive cells, TIM-3 was the most frequently expressed molecule (Fig. 1B), while among the double-positive cells, PD-1^+TIM-3^+ T cells were predominant (Fig. 1C). Among the triple-positive cells, PD-1^+TIM-3^+LAG-3^+ cells represented the largest proportion followed by PD-1^+TIM-3^+CTLA-4^+ cells (Fig. 1D).

We further compared the proportions of $CD4^+$ and $CD8^+$ T cells expressing multiple checkpoint molecules between healthy and EBL cattle on an individual basis. In both $CD4^+$ and $CD8^+$ T-cell populations, the proportion of PD-1^+TIM-3^+ cells was significantly higher in EBL cattle than in healthy cattle (Fig. 2A, B). Consistent with a previous study,[17] the populations of PD-1^+LAG-3^+ cells were higher in $CD4^+$ and $CD8^+$ T cells from EBL cattle (Figs S3B and S4B). Additionally, the proportions of PD-1^+TIM-3^+CTLA-4^+ cells and PD-1^+TIM-3^+LAG-3^+ cells were markedly elevated in $CD4^+$ and $CD8^+$ T cells from EBL cattle (Fig. 2C, D). Notably, the proportion of quadruple-positive cells was significantly higher in $CD8^+$ T cells from EBL cattle (Fig. 2E). These results indicate that peripheral T cells in EBL cattle show upregulation of multiple immune checkpoint molecules, suggesting the induction of advanced T-cell exhaustion.

Significant alterations in the expression profile of immune checkpoint molecules in lymph nodes and tumor tissues of EBL cattle

We also analyzed the lymphomas formed in the lymph nodes and non-lymphoid organs from healthy and EBL cattle. The expression profile of the immune checkpoint molecules in $CD4^+$ and $CD8^+$ T cells from these tissues exhibited more dramatic changes compared with those in the peripheral blood (Fig. 1A, 3A). In the lymph nodes of healthy cattle, $CD4^+$ and $CD8^+$ T cells that did not express immune checkpoint molecules represented the largest proportion, followed by those that expressed single-positive, double-positive, triple-positive, and quadruple-positive cells (Fig. 3A). In contrast, in lymphoma tissues of EBL cattle, double-positive cells were the most abundant in $CD4^+$ and $CD8^+$ T cells, followed by single-positive, negative, triple-positive, and quadruple-positive cells (Fig. 3A). Meanwhile, this pattern differs from that in the peripheral blood, indicating increased co-expression of immune checkpoint molecules in lymphomas of EBL cattle. Among the single-positive cells, TIM-3^+ and PD-1^+ cells were equally predominant in $CD4^+$ T cells, while more than 90% of the single-positive $CD8^+$ T cells expressed TIM-3 (Fig. 3B). In the double-positive group, PD-1^+TIM-3^+ cells accounted for more than 80% of both $CD4^+$ and $CD8^+$ T-cell populations (Fig. 3C). Among triple-positive cells, PD-1^+TIM-3^+LAG-3^+ cells were the most predominant, followed by PD-1^+TIM-3^+CTLA-4^+ cells (Fig. 3D), similar to the pattern observed in peripheral blood (Fig. 1A).

When the proportions of cells expressing multiple immune checkpoint molecules between healthy and EBL cattle were compared, the proportion of PD-1^+TIM-3^+ cells was significantly higher in both $CD4^+$ and $CD8^+$ T cells in lymph nodes from EBL cattle compared to that in healthy cattle (Fig. 4A, B); this was more pronounced in lymphomas formed in non-lymphoid organs (Fig. 4A, B). Consistent with the observations in peripheral blood, the expression levels of LAG-3 and CTLA-4 were higher in PD-1^+TIM-3^+ cells in EBL cattle despite a smaller population (Figs S5 and S6). Furthermore, the proportion of PD-1^+TIM-3^+LAG-$3^+$$CD4^+$ T cells was higher in EBL cattle, whereas both PD-1^+TIM-3^+CTLA-4^+ $CD8^+$ and PD-1^+TIM-3^+LAG-$3^+$$CD8^+$ T cells were markedly more frequent in EBL cattle (Fig. 4C, D). Notably, quadruple-positive cells were also significantly more frequent in $CD8^+$ T cells, but not in $CD4^+$ T cells, from EBL cattle (Fig. 4E). Interestingly, in the lymph nodes of EBL cattle, the proportion of PD-1^+TIM-3^+ $CD4^+$ T cells positively correlated with the proportion of $CD79a^+$ B cells and inversely correlated with the proportion of $CD3^+$ T cells, whereas no such significant correlation was observed for PD-1^+TIM-3^+ $CD8^+$ T cells (Fig. S7A–D).

Bovine γδ T cells constitute a substantial proportion of T cells and are the major regulatory subset in cattle.[38,39] Given the reported high proportion of CD8-expressing γδ T cells in bovine tissues,[38] there is a possibility that the $CD8^+$ T-cell population analyzed so far may include γδ T cells. We therefore analyzed the proportion of γδ T cells and the expression status of immune checkpoint molecules in the lymph nodes of EBL cattle (Fig. S8A). Compared to γδTCR$^-$$CD4^+$ and γδTCR$^-$$CD8^+$ conventional T cells, γδTCR$^+$ T cells represented a minor population within the lymph nodes (Fig. S8B). In particular, γδTCR$^+$$CD8^+$ T cells were much less abundant than γδTCR$^-$$CD8^+$ T cells in the lymph nodes (Fig. S8C), suggesting that γδ T cells have minimal impact on the analyses of the $CD8^+$ T-cell population above. Expression analysis of immune checkpoint molecules on γδ T cells revealed that PD-1^+TIM-3^+γδ T cells were present, but their proportion within the γδ T-cell population was not dominant in the lymph nodes of EBL cattle (Fig. S8D–G).

These results indicate that the dual upregulation of PD-1 and TIM-3 is predominantly responsible for inducing T-cell exhaustion during tumorigenesis induced by BLV.

RNA-seq analysis reveals distinct transcriptomic profiles of PD-1^+TIM-3^+ T cells

To investigate the transcriptional changes in PD-1^+TIM-3^+ T cells in EBL cattle, bulk RNA-seq was conducted on sorted DP (PD-1^+TIM-3^+) and non-DP (PD-1^-TIM-3^-, PD-1^+TIM-3^-, or PD-1^-TIM-3^+) fractions of both $CD4^+$ and $CD8^+$ T cells from lymphomas formed in the lymph nodes (Fig. 5A). We identified 693 and 1,093 DEGs ($\log_2$ fold change > 1 and adjusted P-value < 0.05) between DP and non-DP fractions in of both $CD4^+$ and $CD8^+$ T cells, respectively (Fig. 5B). Among DEGs, several immune checkpoint-related genes (*PDCD1*, *TNFRSF18*, *TOX*, *TOX2*, *TIGIT*, *LAG3*, and

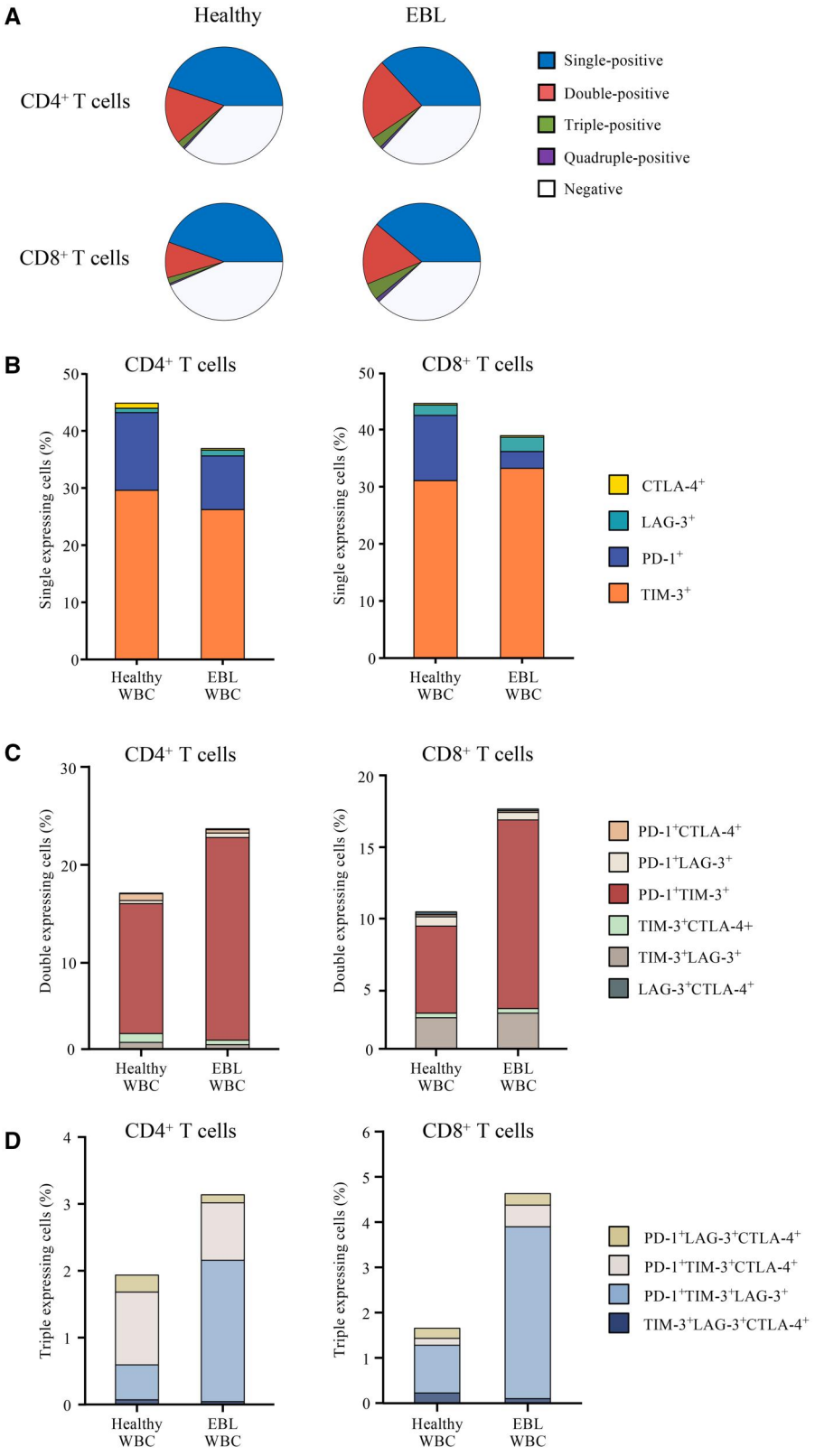

Figure 1. Expression profiling of immune checkpoint molecules in the peripheral blood of healthy and EBL cattle. (A) Pie charts show the average percentage of each cell population within $CD4^+$ or $CD8^+$ T cells in WBCs of healthy ($n = 8$) and EBL cattle ($n = 7$) classified on the basis of the types of positive immune checkpoint molecules in each cell. (B–D) The proportion of cells expressing single-, double-, and triple-positive immune checkpoint molecules in WBCs. In each analysis, cells with other expression patterns were excluded. (B) Cells expressing a single immune checkpoint molecule. (C) Cells expressing 2 immune checkpoint molecules. (D) Cells expressing 3 immune checkpoint molecules. The gating strategy of this assay is provided as Fig. S2A and B.

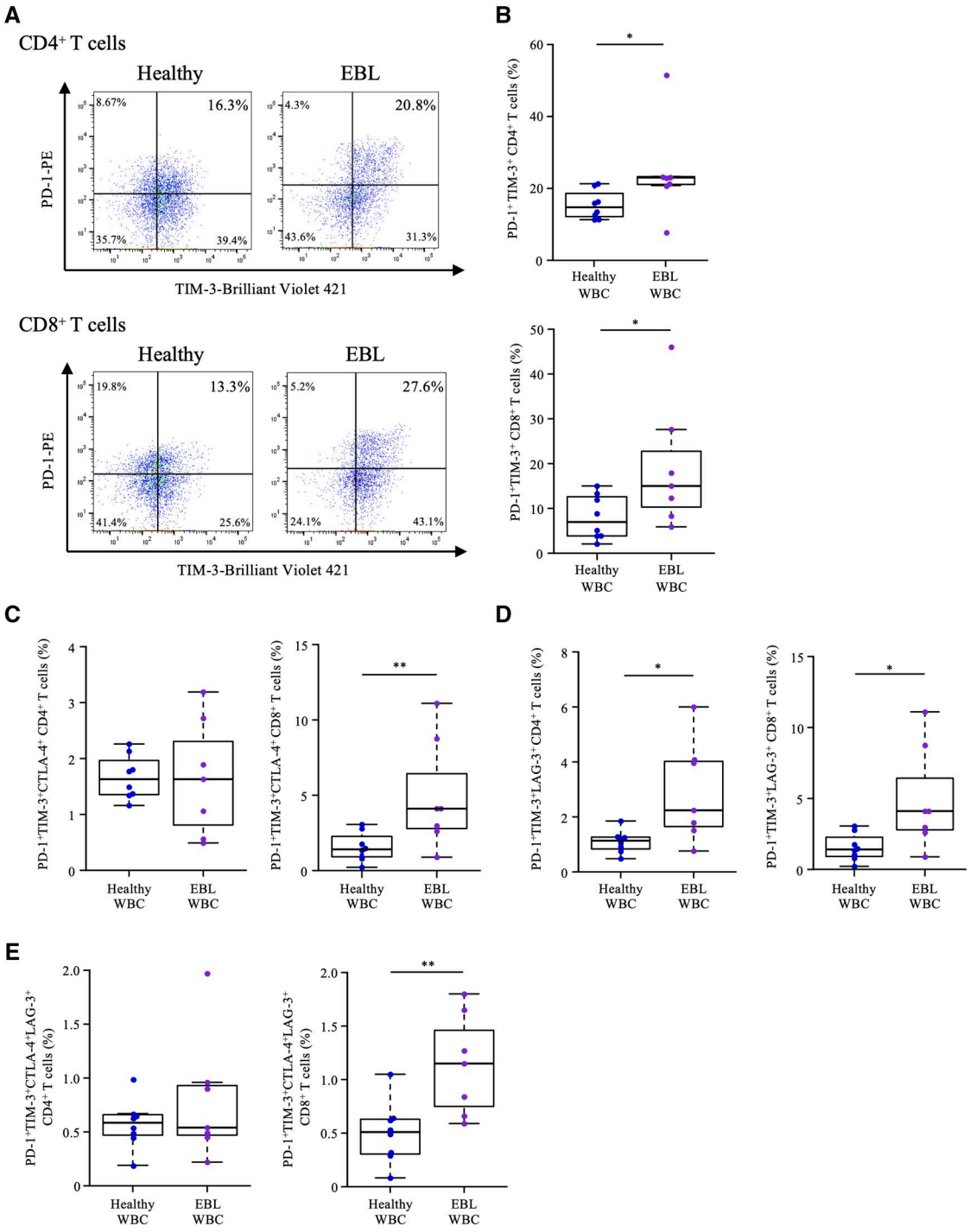

Figure 2. Comparison of immune checkpoint molecule expression on PD-1$^+$TIM-3$^+$ T cells in the peripheral blood of healthy and EBL cattle. (A) Representative flow cytometry plots of PD-1 and TIM-3 expression in CD4$^+$ and CD8$^+$ T cells in WBCs of healthy and EBL cattle. (B–E) Proportions of PD-1$^+$TIM-3$^+$ cells (B), PD-1$^+$TIM-3$^+$CTLA-4$^+$ cells (C), PD-1$^+$TIM-3$^+$LAG-3$^+$ cells (D), or PD-1$^+$TIM-3$^+$CTLA-4$^+$LAG-3$^+$ cells (E) in CD4$^+$ and CD8$^+$ T cells in WBCs of healthy ($n = 8$) and EBL cattle ($n = 7$). The gating strategy of this assay is provided as Fig. S2A and B. *$P < 0.05$; **$P < 0.01$ (Mann–Whitney U test).

CTLA4) were commonly upregulated at the transcriptional level in DP CD4$^+$ and CD8$^+$ T cells (Fig. 5B, C). Notably, DP CD4$^+$ T cells also transcriptionally upregulated genes associated with immune suppression, such as *IL-10*, *CCL4*, and *CD200* (Fig. 5B, C). Conversely, DP CD8$^+$ T cells exhibited marked downregulated expression of genes related to T-cell differentiation and cytokine responses, such as *CCR7*, *TCF7*, *STAT4*, and *IL23R* (Fig. 5B, C). GSEA revealed that pathways related to DNA replication were commonly enriched in both DP CD4$^+$ and DP CD8$^+$ T cells (Fig. 5D). In DP CD8$^+$ T cells, pathways associated with cytokine responses, JAK-STAT signaling, and transforming growth factor-beta (TGF-β) signaling were notably downregulated (Fig. 5D). KEGG pathway analysis was then conducted to further validate and refine the candidate pathways identified through the GSEA results, providing more detailed insights

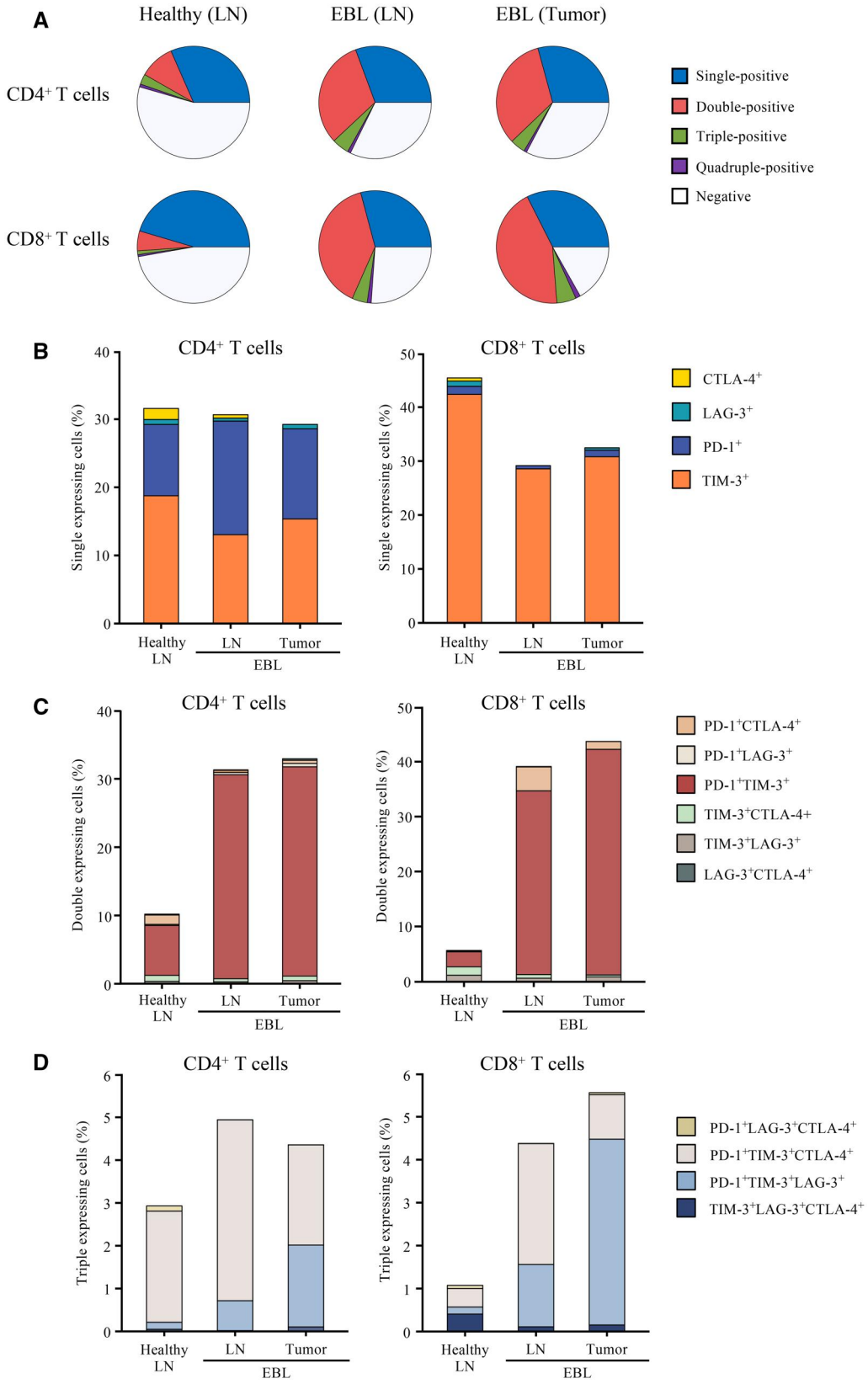

Figure 3. Expression profiling of immune checkpoint molecules in the lymphomas formed in lymph nodes (LNs) and non-lymphoid organs (tumors). (A) Pie charts show the average percentage of each cell population within $CD4^+$ or $CD8^+$ T cells in LNs of healthy ($n = 16$) and EBL cattle ($n = 9$) and tumors of EBL cattle ($n = 6$) classified on the basis of the number of positive immune checkpoint molecules in each cell. (B–D) The proportion of cells expressing single-, double-, or triple-positive immune checkpoint molecules in tissues, with each analysis excluding other expression patterns. (B) Cells expressing a single immune checkpoint molecule. (C) Cells expressing 2 immune checkpoint molecules. (D) Cells expressing 3 immune checkpoint molecules. The gating strategy of this assay is provided as Fig. S2A and B.

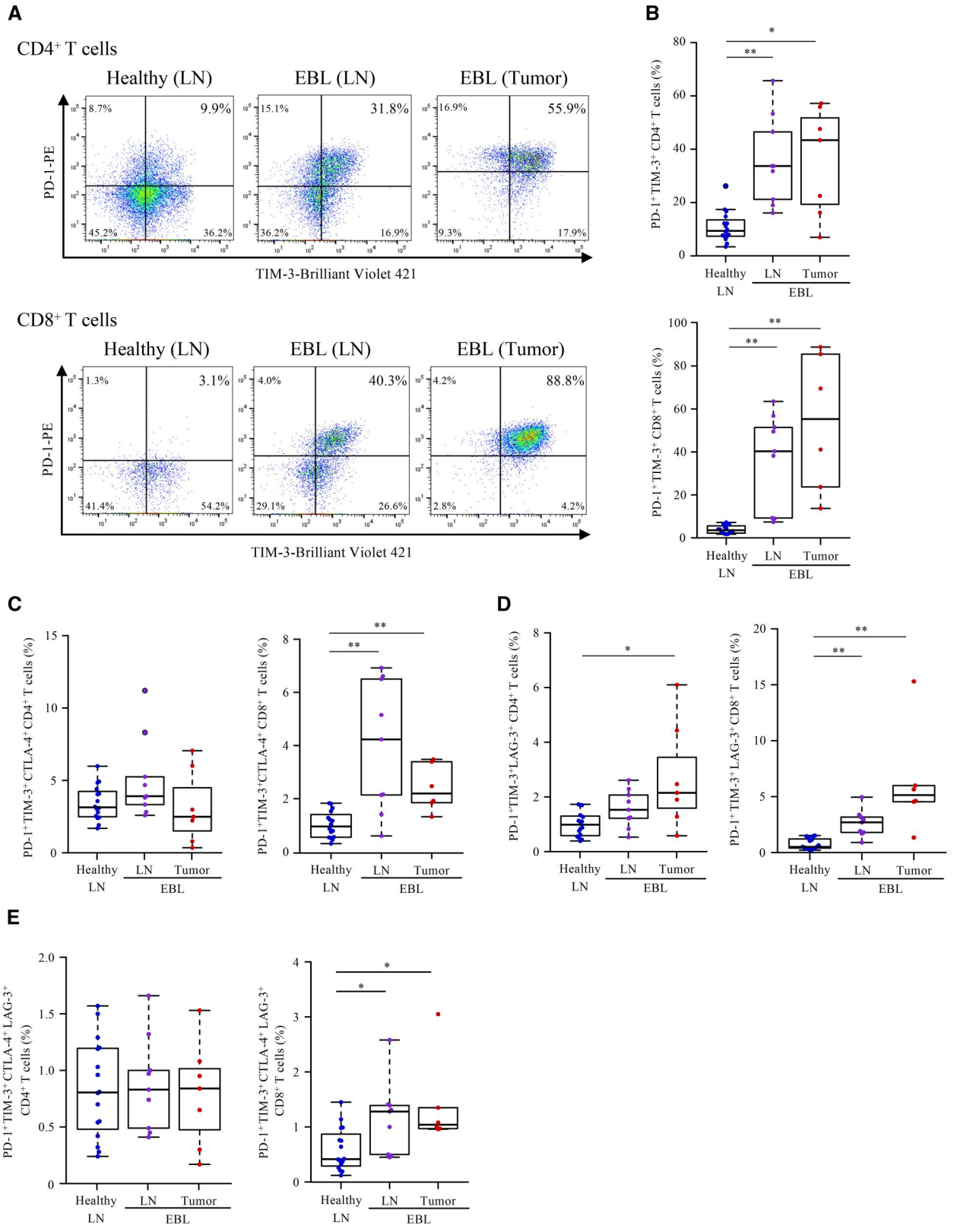

Figure 4. Comparison of immune checkpoint molecule expression on PD-1$^+$TIM-3$^+$ T cells in LNs and tumors from healthy and EBL cattle. (A) Representative flow cytometry plots of PD-1 and TIM-3 expression in CD4$^+$ and CD8$^+$ T cells in LNs of healthy and EBL cattle and tumors of EBL cattle. (B–E) Proportions of PD-1$^+$TIM-3$^+$ cells (B), PD-1$^+$TIM-3$^+$CTLA-4$^+$ cells (C), PD-1$^+$TIM-3$^+$LAG-3$^+$ cells (D), or PD-1$^+$TIM-3$^+$CTLA-4$^+$LAG-3$^+$ cells (E) in CD4$^+$ and CD8$^+$ T cells in LNs of healthy ($n = 16$) and EBL cattle ($n = 9$) and tumors of EBL cattle ($n = 6$). The gating strategy of this assay is provided as Fig. S2A and B. *$P < 0.05$; **$P < 0.01$ (Steel-Dwass test).

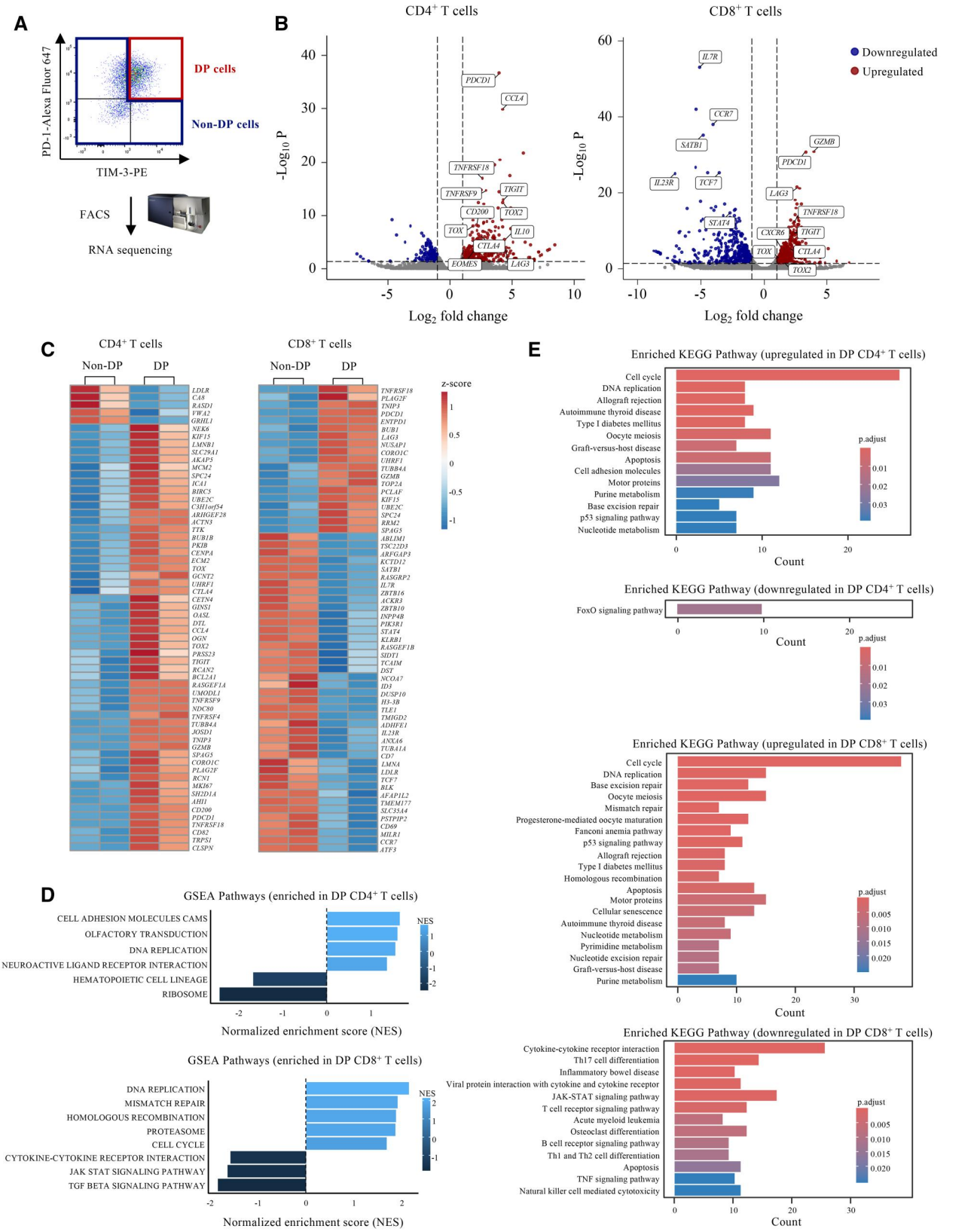

Figure 5. Characterization of PD-1$^+$TIM-3$^+$ T cells using RNA-seq analysis. (A) Gating strategy used for sorting double-positive (DP; PD-1$^+$TIM-3$^+$) and non-double-positive (non-DP; PD-1$^-$TIM-3$^-$, PD-1$^+$TIM-3$^-$, or PD-1$^-$TIM-3$^+$) T cells from LNs of EBL cattle. (B) Volcano plot showing differentially expressed genes between DP and non-DP fractions for CD4$^+$ and CD8$^+$ T cells. Genes with $\log_2$ (fold change) >|1| and adjusted *P*-value <0.05 were considered significant. (C) Heat maps showing the relative expression (z-score) of the top 60 upregulated and downregulated genes in DP CD4$^+$ and CD8$^+$ T cells. (D) Gene Set Enrichment Analysis (GSEA) of DP CD4$^+$ and CD8$^+$ T cells using KEGG pathway gene sets. GSEA was performed by comparing gene expression data from DP T cells with the combined data from other fractions. Pathways with an FDR <0.25 were considered significantly enriched. (E) KEGG pathway analysis illustrating functional enrichment of genes increased or decreased in DP CD4$^+$ and CD8$^+$ T cells, using a significance threshold of adjusted *P*-value <0.05. Data are obtained from 2 independent experiments using LNs from 2 EBL cattle.

into the enriched and suppressed pathways (Fig. 5E). In DP CD4$^+$ T cells, pathways involved in cell proliferation and apoptosis were upregulated, while the FoxO signaling pathway, which plays a critical role in T-cell homeostasis, was the only significantly downregulated pathway. Similarly, in DP CD8$^+$ T cells, pathways promoting cell proliferation were prominently activated. Conversely, in DP CD8$^+$ T cells, pathways related to the interactions between cytokines and their receptors, T-cell differentiation, JAK-STAT signaling, T-cell receptor signaling, and TNF signaling were significantly downregulated, indicating a substantial suppression of genes involved in immune responses.

These findings highlight the distinct gene expression profiles of PD-1$^+$TIM-3$^+$ CD4$^+$ and CD8$^+$ T cells, with shared and unique transcriptomic alterations that may underlie their roles in EBL progression.

PD-1$^+$TIM-3$^+$ T cells exhibit the phenotype of terminally exhausted T cells

To validate and extend the findings from RNA-seq analysis, we characterized the phenotypes of TIM-3$^+$PD-1$^+$ T cells in tumor-forming lymph nodes from EBL-affected cattle by flow cytometry. CD4$^+$ and CD8$^+$ T cells within the tumors were stratified into 3 groups based on PD-1 and TIM-3 expression: PD-1$^-$TIM-3$^-$, PD-1$^+$TIM-3$^-$, and PD-1$^+$TIM-3$^+$ (Fig. 6A). PD-1$^+$TIM-3$^+$ T cells had significantly higher expression levels of immune checkpoint molecules compared to PD-1$^-$TIM-3$^-$ cells (Fig. 6A–E). Interestingly, among PD-1$^+$ T cells, the PD-1$^+$TIM-3$^+$ population exhibited higher PD-1 expression intensity than the PD-1$^+$TIM-3$^-$ population (Fig. 6B), highlighting differences even within PD-1–expressing cells. In addition, the expression levels of LAG-3 and CTLA-4 were also significantly higher in PD-1$^+$TIM-3$^+$ T cells compared to PD-1$^+$TIM-3$^-$ T cells (Fig. 6D, E).

To further characterize PD-1$^+$TIM-3$^+$ T cells, we also analyzed the expression of key transcription factors associated with the maintenance of exhausted T cells, such as Eomes and T-bet, in T cells of lymph nodes from EBL cattle (Fig. 7A, Fig. S9). In both CD4$^+$ and CD8$^+$ T cells, the PD-1$^+$TIM-3$^+$ cells showed high Eomes expression compared to PD-1$^-$TIM-3$^-$ cells, implying a progression toward terminal exhaustion (Fig. 7B). Meanwhile. low T-bet expression was observed in the PD-1$^+$TIM-3$^+$ cells, further supporting the possibility that these double-positive cells have weaker effector functions (Fig. 7C). To gain additional insight into the phenotype of PD-1$^+$TIM-3$^+$ T cells, we stratified T cells into 3 groups based on PD-1 expression levels: PD-1^{neg}, PD-1^{int}, and PD-1^{high} (Fig. S10A). PD-1^{high} CD4$^+$ and CD8$^+$ T cells exhibited higher expression levels of TIM-3 than the PD-1^{neg} and PD-1^{int} subsets (Fig. S10B). When comparing the expression of Eomes and T-bet among these 3 groups, the expression level of Eomes increased along with the expression intensity of PD-1, while the expression level of T-bet decreased (Fig. S10C, D). We also examined the expression of T-cell activation markers, CD69 and CD25 (Fig. 7D, Fig. S11). Similarly, in both CD4$^+$ and CD8$^+$ T cells, the PD-1$^+$TIM-3$^+$ cells showed high expression of CD69 and CD25 in the lymph nodes of EBL cattle (Fig. 7E–G).

These findings indicate that PD-1$^+$TIM-3$^+$ T cells exhibit the phenotype of terminally exhausted T cells, although they express activation markers, presumably owing to persistent antigen stimulation during BLV infection and tumorigenesis.

Effector immune response is impaired in PD-1$^+$TIM-3$^+$ T cells

Finally, we also assessed the status of the effector function of PD-1$^+$TIM-3$^+$ T cells from EBL cattle by assessing their cytokine production in response to stimulation. Lymphocytes from lymphomas formed in the lymph nodes of EBL cattle were sorted into DP and non-DP fractions in both CD4$^+$ and CD8$^+$ T cells. The sorted cells were then cultured with anti-CD3 and anti-CD28 mAbs for 3 d, and IFN-γ production was evaluated in the supernatants (Fig. 8A). In CD4$^+$ T cells, the stimulation of non-DP cells resulted in increased IFN-γ production, while that in DP cells resulted in minimal increases in IFN-γ levels (Fig. 8B). Meanwhile, in CD8$^+$ T cells, stimulation did not result in significant increase in IFN-γ production in either the DP or non-DP fractions (Fig. 8B). We then conducted a similar experiment with stronger stimulation using PMA and ionomycin. Both CD4$^+$ and CD8$^+$ T cells showed increased IFN-γ production in response to the stimulation in EBL #1 (Fig. 8C). Notably, DP cells exhibited significantly lower IFN-γ production compared with non-DP cells in both cases (EBL #1 and #2, Fig. 8C). These data indicate that PD-1$^+$TIM-3$^+$ T cells in EBL cattle exhibit reduced responsiveness to immune-activating stimulation, reflecting severe T-cell dysfunction in EBL.

Discussion

This study revealed that T cells co-expressing multiple immune checkpoint molecules, specifically PD-1 and TIM-3, are predominant in EBL cattle and exhibit characteristics of terminal exhaustion. Additionally, these cells have reduced IFN-γ production, underscoring their impaired functionality in EBL. Our results are expected to influence future research aimed at developing novel therapeutic strategies targeting PD-1 and TIM-3 to control BLV infection.

By utilizing multiplex flow cytometry to simultaneously assess PD-1, TIM-3, CTLA-4, and LAG-3, we comprehensively examined their co-expression patterns in EBL cattle and finally revealed the full profile of exhausted T cells during tumorigenesis. (Figs. 1–4). Unlike prior studies that focused on individual immune checkpoint molecules,[10–17]) this study showed that co-expression of multiple immune checkpoint molecules becomes more pronounced as the disease progresses. Notably, the proportion of single-positive cells did not differ significantly in EBL cattle (Figs. 1A, 3A). Instead, co-expression of PD-1 and TIM-3, along with other immune checkpoint molecules, became more predominant (Figs. 1C, 3C), which is aligned with reports of increased expression of PD-1$^+$TIM-3$^+$ exhausted T cells in cancer patients and an LCMV-infected mouse model.[40,41] Our results have also allowed us to gain novel insights into the potential application of immune checkpoint blockade therapy in BLV infection. A previous study on BLV-infected cattle reported that the dual blockade of PD-L1 and TIM-3 enhances antiviral responses in peripheral immune cells from BLV-infected cattle.[14] Our findings emphasize the potential of a therapeutic strategy that targets multiple immune checkpoints, especially PD-1/PD-L1 and TIM-3. Since sorted PD-1$^+$TIM-3$^+$ T cells are no longer in contact with their ligands expressed by tumor cells, the establishment of a coculture system with autologous tumor cells will enable functional analyses of these subsets, including their response to checkpoint blockade. These studies, along with further animal experiments, will

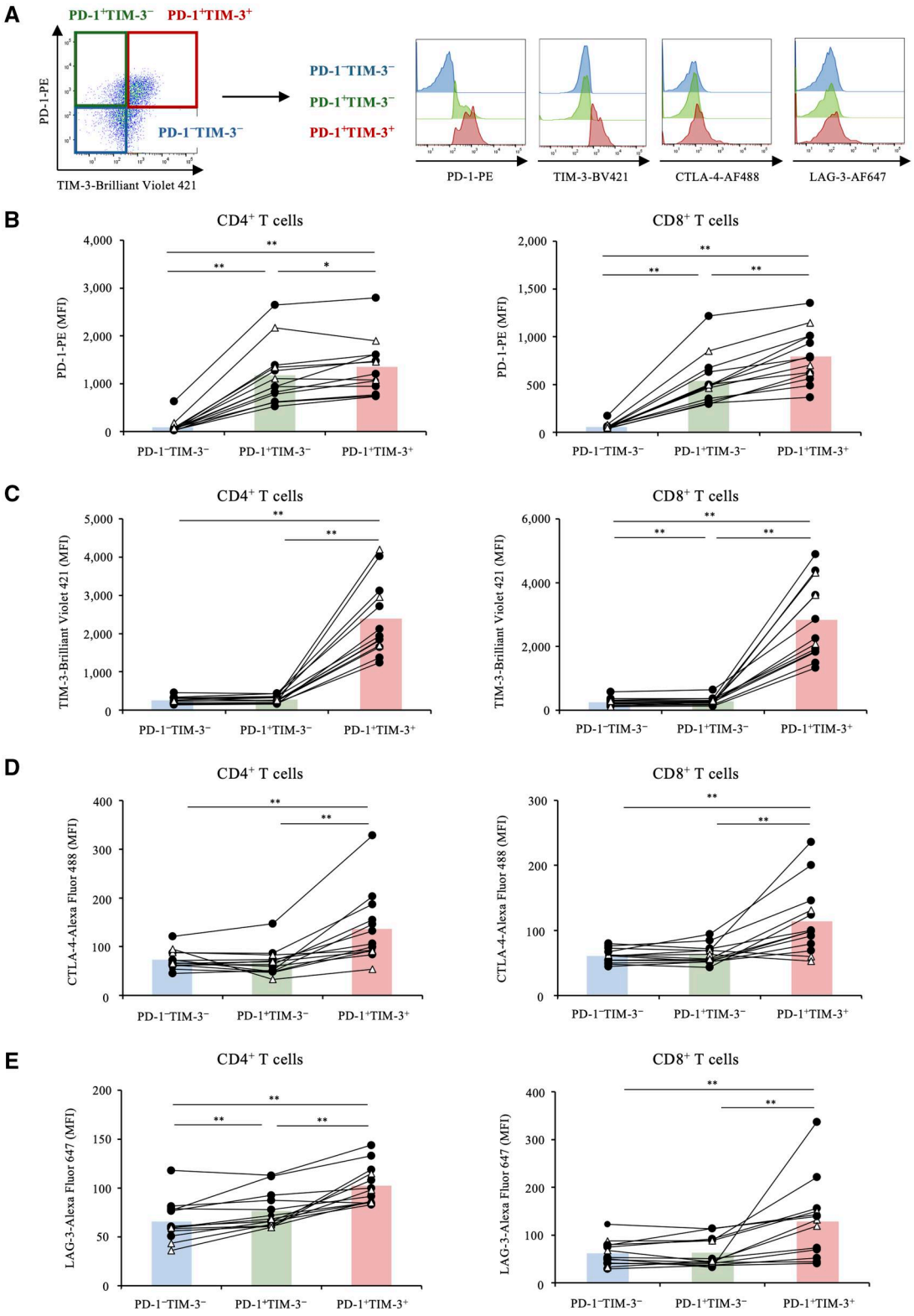

Figure 6. Comparison of immune checkpoint molecule expression levels in CD4$^+$ and CD8$^+$ T cells based on PD-1 and TIM-3 expression. (A) Gating strategy for CD4$^+$ or CD8$^+$ T cells, classified into 3 groups based on PD-1 and TIM-3 expression: PD-1$^+$TIM-3$^+$, PD-1$^+$TIM-3$^-$, and PD-1$^-$TIM-3$^-$. Representative histograms showing mean fluorescent intensity (MFI) for PD-1, TIM-3, CTLA-4, and LAG-3 in each population are included. (B–E) Dot plots comparing the MFI of (B) PD-1, (C) TIM-3, (D) CTLA-4, and (E) LAG-3 among the 3 groups. In each panel, the left graph shows CD4- T cells and the right graph shows CD8- T cells. Data points from the same individual are connected by lines. Dot shapes indicate lymphoma localization: black circles represent lymph nodes, and white triangles represent other organs. Bar plots overlaying the dot plots show the mean MFI for each group. $*P < 0.05$; $**P < 0.01$ (Friedman test followed by the Wilcoxon signed-rank test).

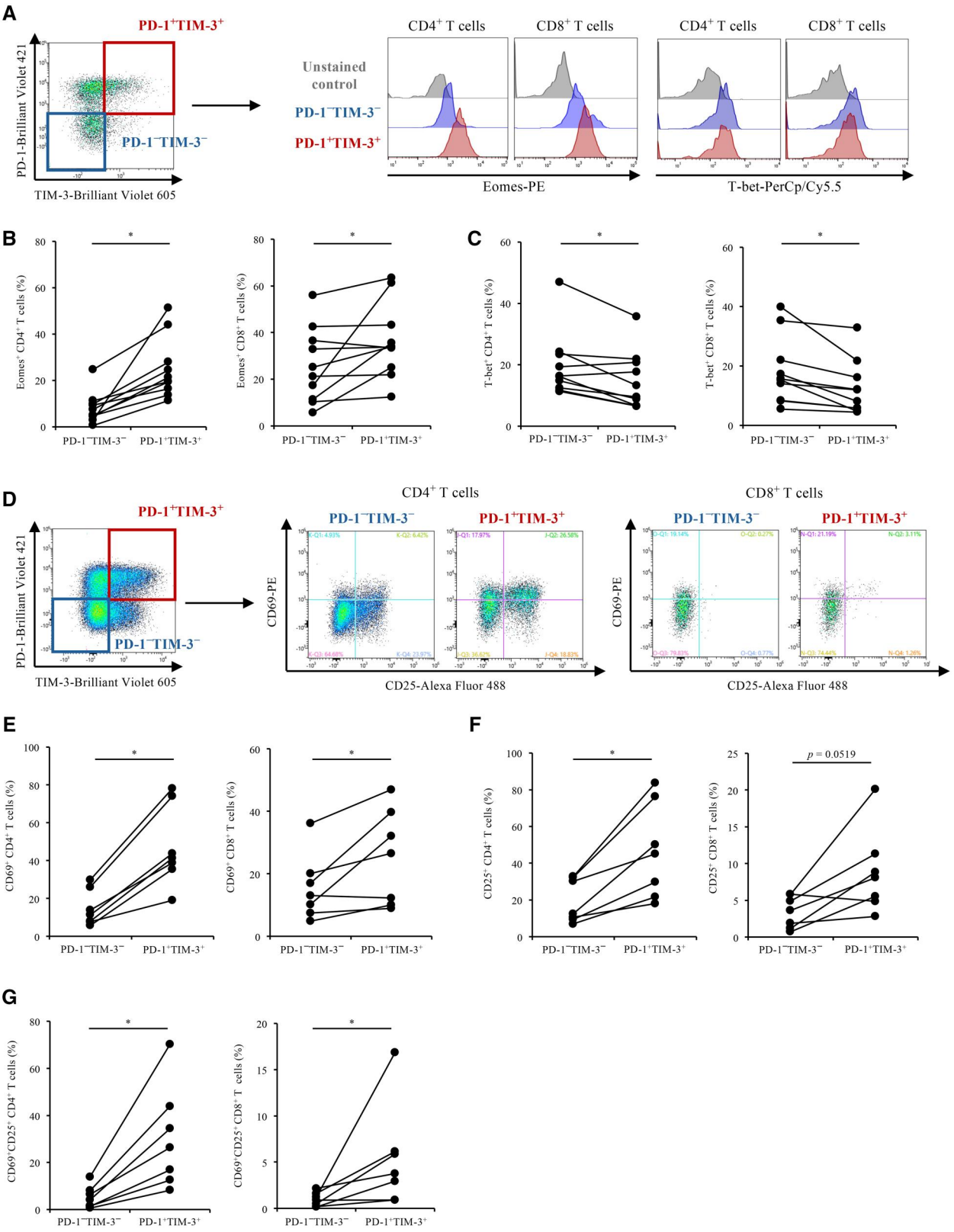

Figure 7. Expression analysis of markers of terminal exhaustion and activation in PD-1$^+$TIM-3$^+$ T cells of EBL cattle. (A) Representative flow cytometry histograms showing the expression of transcription factors Eomes and T-bet in PD-1$^+$TIM-3$^+$ and PD-1$^-$TIM-3$^-$ cell fractions in CD4$^+$ and CD8$^+$ T cells from LNs of EBL cattle. (B, C) Comparison of Eomes (B) and T-bet (C) expression across the cell fractions from LNs of EBL cattle ($n = 10$). (D) Representative flow cytometry plots showing the expression of the activation markers CD69 and CD25 in PD-1$^+$TIM-3$^+$ and PD-1$^-$TIM-3$^-$ cell fractions in CD4$^+$ and CD8$^+$ T cells from LNs of EBL cattle. (E, F) Comparison of CD69 (E) and CD25 (F) expression across the cell fractions from LNs of EBL cattle ($n = 7$). (G) Comparison of the proportions of CD69$^+$CD25$^+$ cells across the cell fractions from LNs of EBL cattle ($n = 7$). The gating strategies of these assays were provided as Figs S8 and S9. *$P < 0.05$ (Wilcoxon signed-rank test).

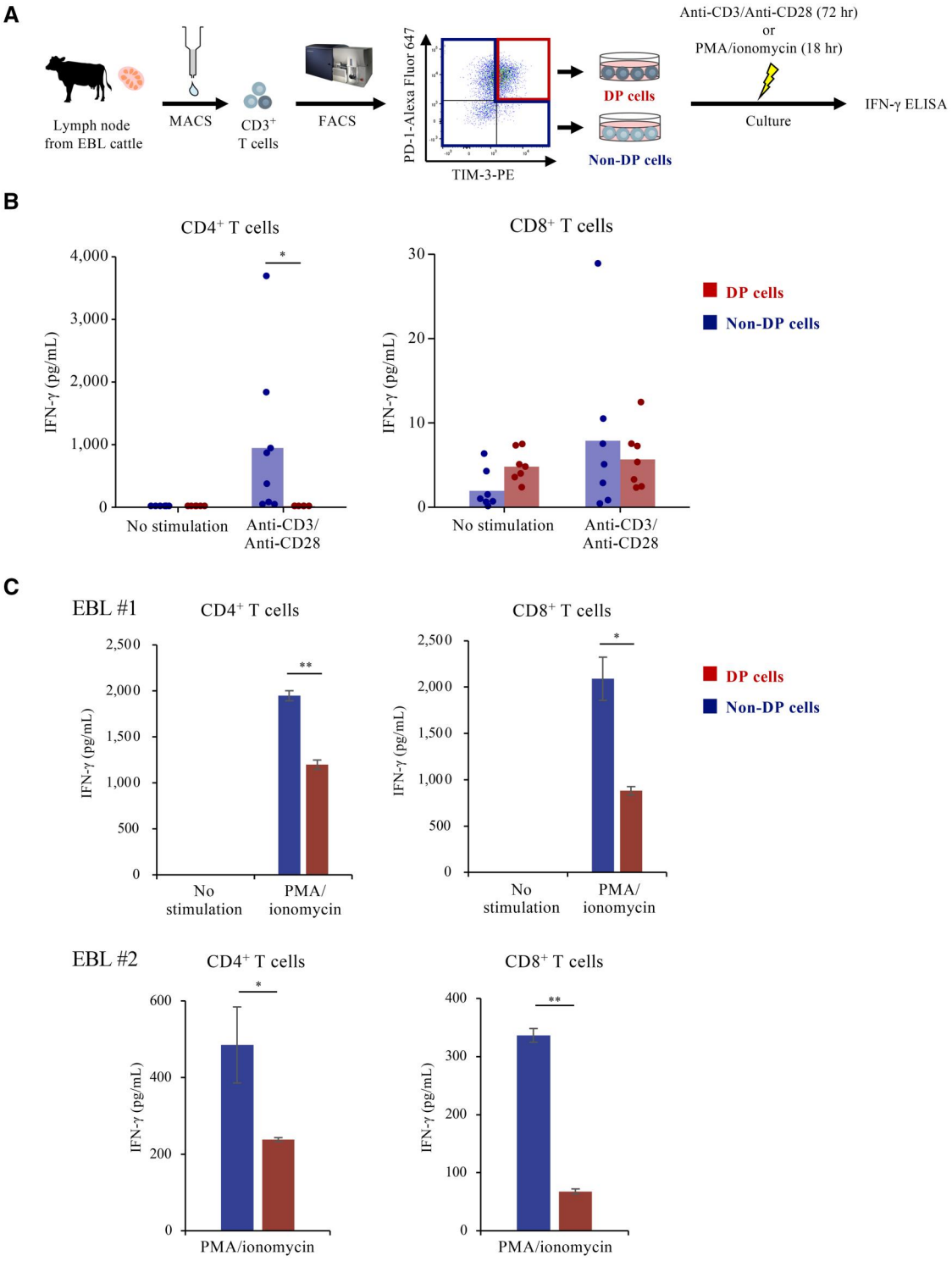

Figure 8. Functional analysis of PD-1$^+$TIM-3$^+$ T cells isolated from EBL cattle. (A) Outline of the cell sorting and the functional analysis. CD3$^+$ T cells were enriched from single-cell suspension of the LN tissues from EBL cattle using magnetic sorting and then sorted into the following 2 populations based on PD-1 and TIM-3 expression for both CD4$^+$ and CD8$^+$ T-cell subsets: double-positive (DP; PD-1$^+$TIM-3$^+$) cells and non-DP (PD-1$^-$TIM-3$^-$, PD-1$^+$TIM-3$^-$, and PD-1$^-$TIM-3$^+$) cells by flow cytometry. The sorted cells were cultivated with stimulations to test the secretion of IFN-γ by ELISA. (B) The sorted DP and non-DP cells (1×10^5 cells/well) from CD4$^+$ ($n = 8$) and CD8$^+$ T-cell subsets ($n = 7$) of EBL cattle were stimulated with or without anti-CD3 and anti-CD28 mAbs (1 μg/mL each) in duplicate for 72 h, and IFN-γ production in the supernatant was evaluated by ELISA. $^*P < 0.05$ (Wilcoxon signed-rank test). (C) The sorted DP and non-DP fractions of CD4$^+$ and CD8$^+$ T cells (1×10^5 cells/well) from 2 individual EBL cattle (#1 and #2) were cultured in triplicate under the stimulation with PMA (20 ng/μL) and ionomycin (1 μg/mL) for 18 h, and IFN-γ production in the supernatant was evaluated by ELISA. The mean values of triplicates are shown in the bar. $^*P < 0.05$, $^{**}P < 0.01$ (paired Student's *t* test).

help determine the optimal combinations for immunotherapy against BLV infection.

Immunological studies in EBL have mostly focused on peripheral blood, while detailed research on tumors and lymph nodes is scarce.[11,14] Herein, we compared the expression profiles of T cells in peripheral blood and lymphomas formed in lymph nodes and non-lymphoid organs, allowing for a direct evaluation of the T-cell phenotype across these tumor tissues.

Our results showed those similar levels of T-cell exhaustion occurred in lymphomas, but this was more advanced exhaustion compared with peripheral blood (Figs. 1–4). This suggests that exhaustion may be more pronounced in the tumor microenvironment (TME) owing to the high density of BLV-infected B cells, resulting in persistent antigenic stimulation. Additionally, we noted the high expression of activation markers CD69 and CD25 in PD-1$^+$TIM-3$^+$ T cells (Fig. 7D–G), which may reflect the persistent antigenic stimulation from BLV-infected B cells in the TME, particularly within the lymph nodes. This is also supported by the findings that the proportion of PD-1$^+$TIM-3$^+$CD4$^+$ T cells correlated with the B-cell population (Fig. S7). Moreover, increased expression of CD69 has been observed in terminally exhausted T cells and is associated with reduced T-bet expression and enhanced Eomes expression, suggesting a potential role for CD69 in the differentiation process of terminally exhausted T cells.[42] Additionally, γδ T cells in the lymphoma tissues were found to co-express PD-1 and TIM-3, further suggesting that γδ T cells may also undergo exhaustion in the TME (Fig. S8D–G). To entirely reveal the mechanisms underlying the severe exhaustion observed in the lymphoma tissues of EBL, characterizing the TME is warranted and may involve the creation of an immunosuppressive environment.

In humans and mice, the TME is formed by various immunosuppressive cells, including regulatory T cells (Tregs) and tumor-associated macrophages (TAMs).[43,44] Tregs suppress effector T-cell activation by releasing inhibitory cytokines, including IL-10 and TGF-β.[43] TAMs, which are typically polarized toward an M2 phenotype in tumors, secrete IL-10, TGF-β, and arginase-1, which inhibit T-cell function and promote tumor progression.[44] Consistently, the RNA-seq analysis in this study revealed increased expression of *IL-10* in PD-1$^+$TIM-3$^+$CD4$^+$ T cells (Fig. 5B, C), which further supportes the formation of immunosuppressive environment within tumors in EBL cattle. Additionally, PD-1$^+$TIM-3$^+$CD4$^+$ T cells exhibited elevated expression of *CCL4*, a chemokine reported to be involved in TAM recruitment,[45] and *CD200*, which has been associated with suppressive TME formation, particularly in PD-1^{hi} CD200^{hi} CD4$^+$ T cells.[46] Furthermore, pathway analysis revealed that PD-1$^+$TIM-3$^+$CD4$^+$ T cells are characterized by enhanced cell survival and maintenance, associated with increased activity in cell cycle- and DNA replication-related pathways, while exhibiting reduced effector functions. These findings suggest that PD-1$^+$TIM-3$^+$CD4$^+$ T cells may actively contribute to the establishment of an immunosuppressive TME by promoting TAM recruitment and enhancing inhibitory signaling pathways rather than supporting effector immune responses.

In this study, we have successfully clarified the phenotype and differentiation state of exhausted T cells by the combination of multicolor flow cytometric assays and RNA-seq analysis of EBL cattle, which was not possible in our previous studies.[10–17] Thymocyte selection-associated HMG box (TOX) is a transcription factor required to regulate the differentiation of terminally exhausted T cells.[47,48] In EBL cattle, both PD-1$^+$TIM-3$^+$CD4$^+$ and PD-1$^+$TIM-3$^+$CD8$^+$ T cells showed higher expression *TOX* in transcription level (Fig. 5B, C). In addition, expression levels of the transcription factor Eomes, which plays a significant role in the upregulation of immune checkpoint molecules and the differentiation of terminally exhausted T cells,[30] was increased in both PD-1$^+$TIM-3$^+$CD4$^+$ and PD-1$^+$TIM-3$^+$CD8$^+$ T cells of EBL cattle (Fig. 5B). These data support the notion that the majority of both CD4$^+$ and CD8$^+$ T-cell subsets appear to be in a state of terminal exhaustion in the lymphoma tissue of EBL. However, a detailed comparison of the RNA-seq and flow cytometric datasets for CD4$^+$ and CD8$^+$ T cells in EBL cattle suggests that the mechanism of terminal exhaustion seems to be different between CD4$^+$ and CD8$^+$ T cells, reflecting potentially different pathways or regulatory processes in their exhaustion. Specifically, CD8$^+$ T cells showed higher co-expression of multiple immune checkpoint molecules than CD4$^+$ T cells in EBL cattle (Figs. 3, 4, Fig. S8F, G). T cell factor-1 (TCF-1), encoded by the *TCF7* gene, is a critical factor for the induction and maintenance of progenitor-like exhausted CD8$^+$ T cells in mice.[49] The significant decrease of *TCF7* expression in PD-1$^+$TIM-3$^+$CD8$^+$ T cells of EBL cattle (Fig. 5B, C) suggests a transition away from a progenitor-like exhausted state toward a terminally exhausted phenotype in CD8$^+$ T cells. Additionally, PD-1$^+$TIM-3$^+$CD8$^+$ T cells exhibited a notable downregulation of *IL7R* and *CCR7*, critical markers for the maintenance of memory T cells and tissue trafficking.[50] The downregulation of these molecules, coupled with pathway analysis indicating reduced Th1/Th2 differentiation, highlights a shift away from naive or memory phenotypes and supports the notion of terminal exhaustion. Furthermore, decreased expression of *IL23R* and *STAT4*, key mediators of cytokine responses and T-cell differentiation,[51] underscores the diminished functional capacity of PD-1$^+$TIM-3$^+$CD8$^+$ T cells in cytokine-driven immune responses. These findings collectively suggest that PD-1$^+$TIM-3$^+$CD8$^+$ T cells of EBL cattle have not only lost their effector capability but have also transitioned into a terminally exhausted state. By considering these transcription factors and other related factors, we may precisely understand the state of T-cell exhaustion.

Our results demonstrate a marked upregulation of PD-1 and TIM-3 expression in EBL tumors compared with CTLA-4 and LAG-3, suggesting that these molecules play a significant role not only in T-cell exhaustion but also in immune suppression in cattle. PD-1 and TIM-3 are known to suppress T-cell function following prolonged antigen exposure, and their co-expression is strongly associated with T-cell exhaustion in thyroid cancer patients.[41] Furthermore, PD-1 and TIM-3 are highly upregulated in response to persistent antigenic stimulation during viral infections and cancer, contributing to impaired T-cell function and reduced cytokine production.[52,53] Galectin-9, which is a ligand for TIM-3, may also bind to PD-1 and participate in the differentiation of exhausted T cells.[54] Therefore, PD-1 and TIM-3 may play a crucial role in T-cell exhaustion through their cross talk mechanisms. In contrast, CTLA-4 mostly functions in the early stages of T-cell priming by competing with B7 molecules,[55] whereas LAG-3 modulates early immune responses through its interaction with MHC class II.[56] The signaling pathways of LAG-3 are complex, and it is thought to work in concert with other checkpoint molecules.[56,57] Additionally, PD-1 and TIM-3 are reported to be epigenetically regulated through mechanisms involving DNA methylation and histone modifications, which may explain their preferential upregulation.[58] As this study focused on only EBL, which is the terminal stage of BLV infection, changes in the expression profiles of PD-1, TIM-3, CTLA-4, and LAG-3 over the course of infection as well as the upregulation of PD-1 and TIM-3 were not evaluated. Future studies on the longitudinal dynamics of

PD-1 and TIM-3 expression across different stages of BLV infection will be critical to further clarify the mechanisms driving T-cell exhaustion.

In conclusion, this study provides novel insights into the mechanisms of T-cell exhaustion in BLV infection and emphasizes the pivotal role of PD-1 and TIM-3. Our findings indicate that targeting these molecules by antibody therapies could be a promising approach for treating BLV infection. Future research may identify the optimal therapies for BLV infection, ultimately contributing to the eradication of BLV and the advancement of cattle health worldwide.

Acknowledgments

We are grateful to the staff of Hokkaido Hayakita Meat Inspection Center and Field Science Center for Northern Biosphere, Hokkaido University, for their cooperation in sample collection. We thank Enago (http://www.enago.jp) for the English language review. The authors have no conflicts of interest to declare.

Author contributions

H.N. performed the experiments, analyzed the data, and wrote the manuscript. S.K. and T.O. conceived of this study, designed the experiments, analyzed the data, and revised the manuscript. W.T., M.I., K.M., and K.W. contributed to the execution of the specific experiments. K.K. and M.S. performed the clinical diagnosis and provided intellectual input and field samples. N.M. assisted in the immunological experiments and data analysis and revised the manuscript. Y.K. and Y.S. provided intellectual input, laboratory materials, and reagents. S.M. and K.O. assisted in the experimental design and revised the manuscript. All authors reviewed and approved the final manuscript.

Hayato Nakamura (Conceptualization [Supporting], Data curation [Equal], Formal analysis [Lead], Funding acquisition [Supporting], Investigation [Lead], Methodology [Equal], Project administration [Supporting], Software [Lead], Validation [Equal], Visualization [Lead]), Satoru Konnai (Conceptualization [Equal], Data curation [Supporting], Formal analysis [Supporting], Funding acquisition [Lead], Project administration [Equal], Supervision [Equal], Validation [Equal], Visualization [Supporting]), Tomohiro Okagawa (Conceptualization [Equal], Data curation [Equal], Formal analysis [Supporting], Funding acquisition [Supporting], Investigation [Supporting], Methodology [Equal], Project administration [Equal], Software [Supporting], Supervision [Equal], Validation [Equal], Visualization [Supporting]), Naoya Maekawa (Conceptualization [Supporting], Data curation [Supporting], Funding acquisition [Supporting], Methodology [Supporting], Project administration [Supporting], Supervision [Supporting], Validation [Supporting]), Wisa Tiyamanee (Investigation [Supporting], Validation [Supporting], Visualization [Supporting]), Mari Ikehata (Funding acquisition [Supporting], Investigation [Supporting], Validation [Supporting]), Koume Matsubara (Investigation [Supporting], Methodology [Supporting]), Kei Watari (Investigation [Supporting], Resources [Supporting]), Kana Kamitani (Resources [Equal], Validation [Supporting]), Maya Saito (Resources [Equal], Validation [Supporting]), Yukinari Kato (Funding acquisition [Supporting], Resources [Supporting], Validation [Supporting]), Yasuhiko Suzuki (Funding acquisition [Supporting], Project administration [Supporting], Resources [Supporting], Validation [Supporting]), Shiro Murata (Conceptualization [Supporting], Data curation [Supporting], Funding acquisition [Supporting], Project administration [Supporting], Supervision [Supporting], Validation [Supporting]), and Kazuhiko Ohashi (Conceptualization [Supporting], Data curation [Supporting], Funding acquisition [Supporting], Project administration [Equal], Supervision [Equal], Validation [Supporting])

Supplementary material

Supplementary material is available at *The Journal of Immunology* online.

Funding

This work was supported by Japan Society for the Promotion of Science (JSPS) KAKENHI (grant numbers 19KK0172, 22K19232, 23K23768, 23KK0124 [to S.K.], 19K15993, 22K15005, 24K01918 [to T.O.], 24KJ0303 [to H.N.]); grants from the Project of the National Agriculture and Food Research Organization (NARO), Bio-oriented Technology Research Advancement Institution (Research Program on Development of Innovative Technology 26058 BC [to S.K.], Special Scheme Project on Regional Developing Strategy, Grant 16817557 [to S.K.], and Research and Implementation Promotion Program through Open Innovation Grants JPJ011937 [to S.K.]); grants from Ito Memorial Foundation (to S.K.); Regulatory Research Projects for Food Safety, Animal Health and Plant Protection (JPJ008617.17935709 [to S.K.]); grants from the Japan Agency for Medical Research and Development (AMED) (JP223fa627005 [to S.K.] and JP24ama121008 [to Y.K.]); Clinical Research Promotion Fund by Hokkaido University Veterinary Teaching Hospital (to S.K.); the Hokkaido University DX Fellowship (to H.N.); and the World-leading Innovative & Smart Education (WISE) Program from the Faculty of Veterinary Medicine at Hokkaido University (to H.N.). The funders had no role in study design, data collection and analysis, decision to publish, or preparation of the manuscript.

Conflicts of interest

None declared.

Data availability

The data availability statement is included in the manuscript and contains the DDBJ accession number as required.

References

1. Schwartz I et al. In vivo leukocyte tropism of bovine leukemia virus in sheep and cattle. J Virol. 1994;68:4589–4596.
2. Mirsky ML, Olmstead CA, Da Y, Lewin HA. The prevalence of proviral bovine leukemia virus in peripheral blood mononuclear cells at two subclinical stages of infection. J Virol. 1996; 70:2178–2183.
3. Schwartz I, Lévy D. Pathobiology of bovine leukemia virus. Vet Res. 1994;25:521–536.

4. Kabeya H, Ohashi K, Onuma M. Host immune responses in the course of bovine leukemia virus infection. J Vet Med Sci. 2001; 63:703–708.
5. Gillet N et al. Mechanisms of leukemogenesis induced by bovine leukemia virus: prospects for novel anti-retroviral therapies in human. Retrovirology. 2007;4:18.
6. Lv G, Wang J, Lian S, Wang H, Wu R. The global epidemiology of bovine leukemia virus: current trends and future implications. Animals. 2024;14:297.
7. Konnai S, Usui T, Ohashi K, Onuma M. The rapid quantitative analysis of bovine cytokine genes by real-time RT-PCR. Vet Microbiol. 2003;94:283–294.
8. Ohira K et al. Bovine leukemia virus reduces anti-viral cytokine activities and NK cytotoxicity by inducing TGF-β secretion from regulatory T cells. Immun Inflamm Dis. 2016;4:52–63.
9. Konnai S, Murata S, Ohashi K. Immune exhaustion during chronic infections in cattle. J Vet Med Sci. 2017;79:1–5.
10. Ikebuchi R, Konnai S, Sunden Y, Onuma M, Ohashi K. Molecular cloning and expression analysis of bovine programmed death-1. Microbiol Immunol. 2010;54:291–298.
11. Ikebuchi R et al. Blockade of bovine PD-1 increases T cell function and inhibits bovine leukemia virus expression in B cells in vitro. Vet Res. 2013;44:59.
12. Ikebuchi R et al. Increase of cells expressing PD-L1 in bovine leukemia virus infection and enhancement of anti-viral immune responses in vitro via PD-L1 blockade. Vet Res. 2011;42:103.
13. Okagawa T et al. Increased bovine Tim-3 and its ligand expressions during bovine leukemia virus infection. Vet Res. 2012;43:45.
14. Nakamura H et al. Combined immune checkpoint blockade enhances antiviral immunity against bovine leukemia virus. J Virol. 2023;97:e01430-22.
15. Suzuki S et al. Increased expression of the regulatory T cell-associated marker CTLA-4 in bovine leukemia virus infection. Vet Immunol Immunopathol. 2015;163:115–124.
16. Konnai S et al. Enhanced expression of LAG-3 on lymphocyte subpopulations from persistently lymphocytotic cattle infected with bovine leukemia virus. Comp Immunol Microbiol Infect Dis. 2013;36:63–69.
17. Okagawa T et al. Cooperation of PD-1 and LAG-3 in the exhaustion of CD4+ and CD8+ T cells during bovine leukemia virus infection. Vet Res. 2018;49:50.
18. Fromentin R et al. CD4+ T cells expressing PD-1, TIGIT and LAG-3 contribute to HIV persistence during ART. PLoS Pathog. 2016;12:e1005761.
19. Snell LM et al. Overcoming CD4 Th1 cell fate restrictions to sustain antiviral CD8 T cells and control persistent virus infection. Cell Rep. 2016;16:3286–3296.
20. Mollavelioglu B et al. High co-expression of immune checkpoint receptors PD-1, CTLA-4, LAG-3, TIM-3, and TIGIT on tumor-infiltrating lymphocytes in early-stage breast cancer. World J Surg Oncol. 2022;20:349.
21. Nishimori A et al. In vitro and in vivo antivirus activity of an anti-programmed death-ligand 1 (PD-L1) rat-bovine chimeric antibody against bovine leukemia virus infection. PLoS ONE. 2017; 12:e0174916.
22. Okagawa T et al. Anti-bovine programmed death-1 rat–bovine chimeric antibody for immunotherapy of bovine leukemia virus infection in cattle. Front Immunol. 2017;8:650.
23. Sajiki Y et al. Prostaglandin E2–induced immune exhaustion and enhancement of antiviral effects by anti–PD-L1 antibody combined with COX-2 inhibitor in bovine leukemia virus infection. J Immunol. 2019;203:1313–1324.
24. Okagawa T et al. Development of a high-affinity anti-bovine PD-1 rabbit–bovine chimeric antibody using an efficient selection and large production system. Vet Res. 2023;54:82.
25. Koyama S et al. Adaptive resistance to therapeutic PD-1 blockade is associated with upregulation of alternative immune checkpoints. Nat Commun. 2016;7:10501.
26. Woroniecka K et al. T-cell exhaustion signatures vary with tumor type and are severe in glioblastoma. Clin Cancer Res. 2018; 24:4175–4186.
27. Miller BC et al. Subsets of exhausted CD8+ T cells differentially mediate tumor control and respond to checkpoint blockade. Nat Immunol. 2019;20:326–336.
28. Jiang W et al. Exhausted CD8+T cells in the tumor immune microenvironment: new pathways to therapy. Front Immunol. 2021; 11:622509.
29. Kao C et al. Transcription factor T-bet represses expression of the inhibitory receptor PD-1 and sustains virus-specific CD8+ T cell responses during chronic infection. Nat Immunol. 2011; 12:663–671.
30. Intlekofer AM et al. Effector and memory CD8+ T cell fate coupled by T-bet and eomesodermin. Nat Immunol. 2005; 6:1236–1244.
31. Buggert M et al. T-bet and Eomes are differentially linked to the exhausted phenotype of CD8+ T cells in HIV infection. PLoS Pathog. 2014;10:e1004251.
32. McLane LM et al. Role of nuclear localization in the regulation and function of T-bet and Eomes in exhausted CD8 T cells. Cell Rep. 2021;35:109120.
33. Okagawa T et al. Diagnosis and early prediction of lymphoma using high-throughput clonality analysis of bovine leukemia virus-infected cells. Microbiol Spectr. 2022;10:e02595-22.
34. Nishimori A et al. Identification of an atypical enzootic bovine leukosis in Japan by using a novel classification of bovine leukemia based on immunophenotypic analysis. Clin Vaccine Immunol. 2017;24:e00067-17.
35. Okagawa T et al. Bovine immunoinhibitory receptors contribute to suppression of Mycobacterium avium subsp. paratuberculosis-specific T-cell responses. Infect Immun. 2016;84:77–89.
36. Watari K et al. Enhancement of interleukin-2 production by bovine peripheral blood mononuclear cells treated with the combination of anti-programmed death-ligand 1 and cytotoxic T lymphocyte antigen 4 chimeric monoclonal antibodies. J Vet Med Sci. 2022;84:6–15.
37. Niwa H, Yamamura K, Miyazaki J. Efficient selection for high-expression transfectants with a novel eukaryotic vector. Gene. 1991;108:193–199.
38. Baldwin CL, Telfer JC. The bovine model for elucidating the role of γδ T cells in controlling infectious diseases of importance to cattle and humans. Mol Immunol. 2015;66:35–47.
39. Guzman E et al. Bovine γδ T cells are a major regulatory T cell subset. J Immunol. 2014;193:208–222.
40. Sakuishi K et al. Targeting Tim-3 and PD-1 pathways to reverse T cell exhaustion and restore anti-tumor immunity. J Exp Med. 2010;207:2187–2194.
41. Severson JJ et al. PD-1+Tim-3+ CD8+ T lymphocytes display varied degrees of functional exhaustion in patients with regionally metastatic differentiated thyroid cancer. Cancer Immunol Res. 2015;3:620–630.
42. Beltra JC et al. Developmental relationships of four exhausted CD8+ T cell subsets reveals underlying transcriptional and epigenetic landscape control mechanisms. Immunity. 2020;52: 825–841.e8.
43. Strauss L et al. A unique subset of CD4+CD25highFoxp3+ T cells secreting interleukin-10 and transforming growth factor-β1 mediates suppression in the tumor microenvironment. Clin Cancer Res. 2007;13:4345–4354.
44. Han S et al. D-lactate modulates M2 tumor-associated macrophages and remodels immunosuppressive tumor microenvironment for hepatocellular carcinoma. Sci Adv. 2023;9:eadg2697.
45. Kersten K et al. Spatiotemporal co-dependency between macrophages and exhausted CD8+ T cells in cancer. Cancer Cell. 2022; 40:624–638.e9.
46. Wu C et al. PD1hi CD200hi CD4+ exhausted T cells increase immunotherapy resistance and tumour progression by promoting

epithelial-mesenchymal transition in bladder cancer. Clin Transl Med. 2023;13:e1303.
47. Scott AC et al. TOX is a critical regulator of tumour-specific T cell differentiation. Nature. 2019;571:270–274.
48. Page N et al. Expression of the DNA-binding factor TOX promotes the encephalitogenic potential of microbe-induced autoreactive CD8+ T cells. Immunity. 2018;48:937–950.e8.
49. Chen Z et al. TCF-1-centered transcriptional network drives an effector versus exhausted CD8 T cell-fate decision. Immunity. 2019; 51:840–855.e5.
50. Im SJ et al. Defining CD8+ T cells that provide the proliferative burst after PD-1 therapy. Nature. 2016;537:417–421.
51. Gollob JA et al. Impairment of STAT activation by IL-12 in a patient with atypical mycobacterial and staphylococcal infections. J Immunol. 2000;165:4120–4126.
52. Fourcade J et al. Upregulation of Tim-3 and PD-1 expression is associated with tumor antigen–specific CD8+ T cell dysfunction in melanoma patients. J Exp Med. 2010;207:2175–2186.
53. Jin H-T et al. Cooperation of Tim-3 and PD-1 in CD8 T-cell exhaustion during chronic viral infection. Proc Natl Acad Sci USA. 2010;107:14733–14738.
54. Yang R et al. Galectin-9 interacts with PD-1 and TIM-3 to regulate T cell death and is a target for cancer immunotherapy. Nat Commun. 2021;12:832.
55. Chikuma S, Abbas AK, Bluestone JA. B7-independent inhibition of T cells by CTLA-4. J Immunol. 2005;175:177–181.
56. Cai L, Li Y, Tan J, Xu L, Li Y. Targeting LAG-3, TIM-3, and TIGIT for cancer immunotherapy. J Hematol Oncol. 2023; 16:101.
57. De Sousa Linhares A, Leitner J, Grabmeier-Pfistershammer K, Steinberger P. Not all immune checkpoints are created equal. Front. Immunol. 2018;9:1909.
58. Sasidharan Nair V et al. DNA methylation and repressive H3K9 and H3K27 trimethylation in the promoter regions of PD-1, CTLA-4, TIM-3, LAG-3, TIGIT, and PD-L1 genes in human primary breast cancer. Clin Epigenet. 2018;10:78.

The Journal of Immunology, 2025, 00, 1–17
https://doi.org/10.1093/jimmun/vkaf050
Research Article